

SECONDARY BARYON ASYMMETRY IN $\pi^\pm p$ COLLISIONS

G. H. Arakelyan*, C. Merino,[†] and Yu. M. Shabelski**

**Yerevan Physics Institute, Armenia*

E-mail: argev@mail.yerphi.am

[†]Departamento de Física de Partículas, Facultade de Física, and Instituto Galego de Altas Enerxías (IGAE), Universidade de Santiago de Compostela, Galicia, Spain

E-mail: merino@fpaxp1.usc.es

***Petersburg Nuclear Physics Institute, Gatchina, St.Petersburg, Russia*

E-mail: shabelsk@thd.pnpi.spb.ru

Abstract. The process of secondary baryon production in $\pi^\pm p$ collisions at high energies in the central and forward fragmentation regions is considered in the framework of the Quark-Gluon String Model. The contribution of the string-junction mechanism to the baryon production is analysed. The results of numerical calculations are in reasonable agreement with the experimental data on the $\Lambda/\bar{\Lambda}$ and p/\bar{p} asymmetries.

Keywords: baryon, strange baryon, production asymmetry

PACS: PACS.25.75.Dw Particle and resonance production

The Quark-Gluon String Model (QGSM) is based on the Dual Topological Unitarization (DTU) and it describes quite reasonably many features of high energy production processes, both in hadron-nucleon and in hadron-nucleus collisions [1-6]. High energy interactions are considered as taking place via the exchange of one or several Pomerons, and all elastic and inelastic processes result from cutting through or between those exchanged Pomerons [7, 8]. The possibility of different numbers of Pomerons to be exchanged introduces absorptive corrections to the cross-sections which are in agreement with the experimental data on production of secondary hadrons.

Hadrons are composite bound state configurations built up from the quark and gluon fields. In the string models baryons are considered as configurations consisting of three strings attached to three valence quarks and connected in one point that is called string junction (SJ) [9-11], as it is shown in Fig. 1. Thus the SJ mechanism has a nonperturbative origin in QCD. Such baryon structure is also supported by lattice calculations [12].

It is important to understand the role of the SJ mechanism in the dynamics of high energy hadronic interactions, in particular in processes implying baryon number transfer [13-15]. Significant results for hadron-hadron and hadron-nucleus collisions were obtained in [15-22].

In this note we analyse the contribution of the SJ mechanism in the description of the existing data on spectra and on asymmetry of Λ and $\bar{\Lambda}$ and on asymmetry of p and \bar{p} production. We use the same parametrisations of diquark fragmentation functions to baryons and the same Regge trajectory intercepts as in [15-19, 21, 22].

As it is thoroughly known the exchange of one or several Pomerons is one basic

feature of high energy interactions in the frame of QGSM. Each Pomeron corresponds to a cylindrical diagram, and thus when cutting a Pomeron two showers of secondaries are produced [1, 2]. The inclusive spectrum of secondaries is determined by the convolution of diquark, valence, and sea quark distribution functions in the incident particle, $u(x, n)$, with the fragmentation functions of quarks and diquarks into secondary hadrons, $G^h(z)$. All these functions are determined by the corresponding Reggeon intercepts [23].

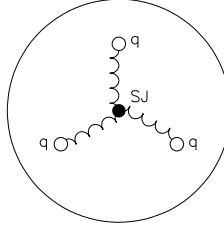


FIGURE 1. Composite structure of a baryon in string model.

The formulas for inclusive spectra, i.e. the Feynman- x distributions, of a secondary hadron h in the QGSM together with the description of high energy experimental data were presented in [1, 5, 15, 18]. The analytical expressions for the complete set of the involved distribution and fragmentation functions are shown in [18].

To produce a secondary baryon in the process of diquark fragmentation three possibilities exist that are shown in Fig. 2. The secondary baryon can consist of: the initial SJ together with two valence and one sea quarks (Fig. 2a), the initial SJ together with one valence and two sea quarks (Fig. 2b), the initial SJ together with three sea quarks (Fig. 2c). The fraction of the incident baryon energy carried by the secondary baryon decreases from case (a) to case (c), whereas the mean rapidity gap between the incident and secondary baryon increases.

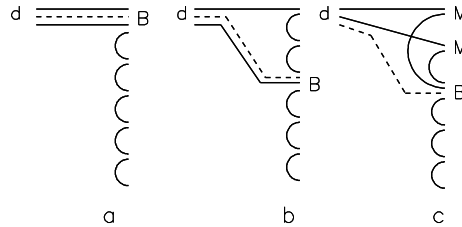


FIGURE 2. QGSM diagrams describing secondary baryon B production by diquark d : (a) initial SJ together with two valence quarks and one sea quark, (b) initial SJ together with one valence quark and two sea quarks, and (c) initial SJ together with three sea quarks.

The diagram of Fig. 2a describes the usual production of the leading baryon on diquark fragmentation. The diagram of Fig. 2b has been used for the description of the baryon number transfer [1, 24], and it also describes the fast meson production by a diquark [23].

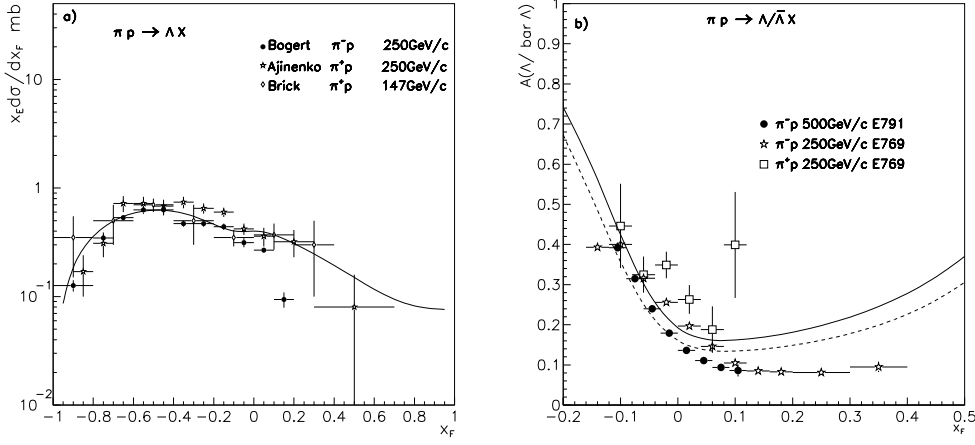


FIGURE 3. The QGSM description of Λ production and of the asymmetry $A(\Lambda/\bar{\Lambda})$ in $\pi^\pm p$ collisions with $\alpha_{SJ} = 0.9$: a) experimental data on the Λ spectrum at $P_{lab} = 147$ GeV/c [27] and $P_{lab} = 250$ GeV/c [28, 29]; b) experimental data on asymmetry data at $P_{lab} = 250$ GeV/c [30] and $P_{lab} = 500$ GeV/c [31]. The solid curves correspond to the value $\delta = 0.32$ and the dashed curve to $\delta = 0.2$.

The contribution of the graph in Fig. 2c to the diquark fragmentation function is the most important for the baryon number transfer to large rapidity distances. This contribution has been determined in [15, 16], and it is proportional to a small coefficient ε (the suppression factor of the process of Fig. 2c compared to those in Figs. 2a and 2b). The formulas for the diquark fragmentation functions corresponding to diagrams on Fig. 2 are the following [15]:

$$G_{uu}^p = G_{ud}^p = a_N z^\beta \left[v_0 \varepsilon (1-z)^2 + v_q z^{2-\beta} (1-z) + v_{qq} z^{2.5-\beta} \right], \quad (1)$$

$$G_{ud}^\Lambda = a_N z^\beta \left[v_0 \varepsilon (1-z)^2 + v_q z^{2-\beta} (1-z) + v_{qq} z^{2.5-\beta} \right] (1-z)^{\Delta\alpha}, \quad G_{uu}^\Lambda = (1-z) G_{ud}^\Lambda. \quad (2)$$

The terms proportional to v_0 , v_q , and v_{qq} correspond to the contributions of Fig. 2a, 2b and 2c, respectively.

The factor z^β is actually $z^{1-\alpha_{SJ}}$, where α_{SJ} is the intercept of the Reggeon trajectory which corresponds to the SJ exchange. As for the factor $z^\beta \cdot z^{2-\beta}$ in the second term, it corresponds to $z^{2(\alpha_R - \alpha_B)}$ [1]. For the third term we have added an extra factor $z^{1/2}$ [15].

The values of the parameters v_0 , v_q , and v_{qq} in Eqs. (1) and (2) are obtained by simple quark combinatorics [15, 25, 26].

In the present calculation, we use the values of parameter $\alpha_{SJ} = 0.9$ and of $\varepsilon = 0.024$, as it was done in [16, 17].

The strange quark suppression factor δ in the model is usually taken for calculations in the interval $\delta \sim 0.2-0.3$. As it was shown in [17], the better agreement of QGSM with experimental data on strange baryon production on nucleus was obtained with $\delta = 0.32$, instead of the previous value $\delta = 0.2$ [15]. In principle we cannot exclude the possibility that the value of δ could be different for secondary baryons and mesons.

The SJ mechanism does not affect the production of antibaryons, so the $\bar{\Lambda}$ spectrum doesn't depend on the value of α_{SJ} , and it has a very small dependence on the strange quark suppression factor δ (see [18, 19]).

In the figures the solid curves correspond to calculations with $\alpha_{SJ} = 0.9$, $\varepsilon = 0.024$, and $\delta = 0.32$. Dashed curves are obtained with the same α_{SJ} and ε , but with $\delta = 0.2$.

The inclusive spectra of Λ in $\pi^\pm p$ collisions at $P_{lab} = 147$ GeV/c [27] and $P_{lab} = 250$ GeV/c [28, 29] together with the model calculation are shown in Fig. 3a. Agreement is reasonably good, and the energy dependence of the model predictions is very weak at these energies.

In Fig. 3b we show the data on the $A(\Lambda/\bar{\Lambda})$ asymmetry

$$A(\Lambda/\bar{\Lambda}) = \frac{N_\Lambda - N_{\bar{\Lambda}}}{N_\Lambda + N_{\bar{\Lambda}}} \quad (3)$$

in πp interactions at $P_{lab} = 250$ GeV/c [30] and $P_{lab} = 500$ GeV/c [31].

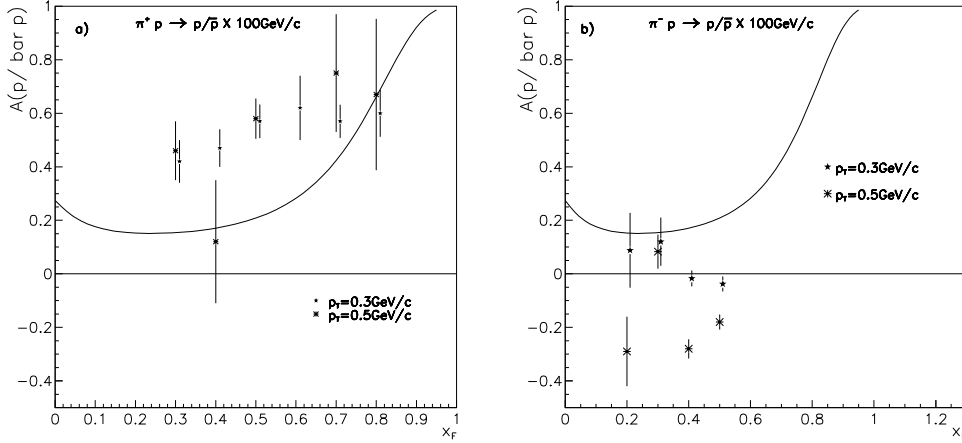


FIGURE 4. The QGSM description of the asymmetry $A(p/\bar{p})$ in π^+p and in π^-p collisions at $P_{lab} = 100$ GeV/c. The solid curve corresponds to SJ with $\alpha_{SJ} = 0.9$.

In the proton fragmentation region the values of $A(\Lambda/\bar{\Lambda})$ are close to unity, and that is natural since a proton fragments into Λ with significantly larger probability than into $\bar{\Lambda}$. In the central and forward fragmentation regions asymmetries are rather small. In principle, there is no reason for a difference in the asymmetry $A(\Lambda/\bar{\Lambda})$ in π^+ and in π^- collisions, since through isotopical reflection the reaction $\pi^+p \rightarrow \Lambda$ becomes $\pi^-n \rightarrow \Lambda$, and vice versa, so the spectra of Λ in π^+p and in π^-p collisions should be similar. The same can be said about $\bar{\Lambda}$ production. Actually in the QGSM frame the asymmetry $A(\Lambda/\bar{\Lambda})$ in π^+p and in π^-p collisions is exactly the same. However, some difference appears in the experimental values of $A(\Lambda/\bar{\Lambda})$, obtained in the same experiment E769 [30].

The inclusive spectra of secondary protons produced in πp collisions at $P_{lab} = 100$ GeV/c [32], together with the corresponding theoretical curves, are presented in Fig. 4a (π^+ beam) and Fig. 4b (π^- beam). As it was already noted, the experimental data [32] contain only inclusive spectra measured at fixed p_T . We calculate the corresponding

asymmetry data where possible. As one can see, the comparison with the data is not good, in particular for π^- beam. Here again the QGSM predicts rather small difference in $A(p/\bar{p})$ for π^+p and π^-p collisions, whereas the experimental behavior of the asymmetry for both beams is very different. The experimental data at $P_{lab} = 175$ GeV/c [32] practically coincide with those in Fig.4 at $P_{lab} = 100$ GeV/c. Possibly the disagreement is in part connected with the fact that in the case of p/\bar{p} asymmetry only data at fixed p_T are available.

In conclusion, the experimental data on high-energy Λ production support the possibility of baryon charge transfer over large rapidity distances. The $\bar{\Lambda}/\Lambda$ asymmetry is provided by SJ diffusion through baryon charge transfer.

To get a good understanding of the dynamics of the baryon charge transfer over large rapidity distances new experimental data in meson and baryon collisions with nucleons and nuclear targets are needed.

ACKNOWLEDGMENTS

The authors are thankful to A. B. Kaidalov and C. Pajares for useful discussions.

This work was supported by Ministerio de Educación by Ciencia of Spain under project FPA2005-01963 and by Xunta de Galicia (Consellería de Educación). The work of Yu.M.Sh. were also supported in part by grant RSGSS-1124.2003.2. G.H.A and Yu.M.Sh. thank the members of the Department of Particle Physics and of the Instituto Galego de Altas Enerxías (IGAE), University of Santiago de Compostela, Galicia, Spain, for their kind hospitality.

REFERENCES

1. A. B. Kaidalov and K. A. Ter-Martirosyan, *Yad. Fiz.* **39**, 1545 (1984); **40**, 211 (1984).
2. A. Capella, U. Sukhatme, C. I. Tan, and J. Tran Thanh Van, *Phys. Rep.* **236**, 225 (1994); A. Capella and J. Tran Thanh Van, *Z. Phys.* **C10**, 249 (1981).
3. A. B. Kaidalov, K. A. Ter-Martirosyan, and Yu. M. Shabelski, *Yad. Fiz.* **43**, 1282 (1986).
4. Yu. M. Shabelski, *Yad. Fiz.* **44**, 186 (1986).
5. A. B. Kaidalov and O. I. Piskunova, *Z. Phys.* **C30**, 145 (1986).
6. G. H. Arakelyan, C. Pajares, and Yu. M. Shabelski, *Z. Phys.* **C73**, 697 (1997).
7. V. A. Abramovsky, V. N. Gribov, and O. V. Kancheli, *Yad. Fiz.* **18**, 595 (1973).
8. K. A. Ter-Martirosyan, *Phys. Lett.* **B44**, 377(1973).
9. X. Artru, *Nucl. Phys.* **B85**, 442 (1975).
10. M. Imachi, S. Otsuki, and F. Toyoda, *Prog. Theor. Phys.* **54**, 280 (1976); **55**, 551 (1976).
11. G. C. Rossi and G. Veneziano, *Nucl. Phys.* **B123**, 507 (1977).
12. V. G. Bornyanov et al., *Usp. Fiz. Nauk* **174**, 19 (2004).
13. D. Kharzeev, *Phys. Lett.* **B378**, 238 (1996).
14. B. Z. Kopeliovich and B. Povh, *Z. Phys.* **C75**, 693, (1997).
15. G. H. Arakelyan, A. Capella, A. B. Kaidalov, and Yu. M. Shabelski, *Eur. Phys. J.* **C26**, 81 (2002).
16. F. Bopp and Yu. M. Shabelski, *Yad. Fiz.* **68**, 2155 (2005); hep-ph/0406158 (2004).
17. F. Bopp and Yu. M. Shabelski, *Eur. Phys. J.* **A28**, 237 (2006); hep-ph/0603193.
18. G. H. Arakelyan, C. Merino, and Yu. M. Shabelski, *Yad. Fiz.* **69**, 884 (2006); hep-ph/0505100.
19. G. H. Arakelyan, C. Merino, and Yu. M. Shabelski, *Yad. Fiz.* **70**, 1110 (2007); hep-ph/0604103.
20. O. I. Piskounova, *Proc. of the PANIC'05*, Santa Fe, October 2005; *Yad. Fiz.* (in press), hep-ph/0604157.

21. G. H. Arakelyan, C. Merino, and Yu. M. Shabelski, Eur. Phys. J. **A31**, 519 (2007); hep-ph/0610264. Proceedings of the IVth International Conference on Quarks and Nuclear Physics, Madrid, Spain, June 5-10, 2006. Springer-Verlag, 2007, p.151.
22. Yu. M. Shabelski, hep-ph/0705.0947.
23. A. B. Kaidalov, Sov. J. Nucl. Phys. **45**, 902 (1987); Yad. Fiz. **43**, 1282 (1986).
24. A. Capella and B. Z. Kopeliovich, Phys. Lett. **B381**, 325 (1996).
25. V. V. Anisovich and V. M. Shekhter, Nucl. Phys. **B55**, 455 (1980).
26. A. Capella and C. A. Salgado, Phys. Rev. **C60**, 054906 (1999).
27. D. Brick et al., Nucl. Phys. **B164**, 1 (1980).
28. I. V. Ajinenko et al., EHS-NA22 Collaboration, Z. Phys. **C44**, 573 (1989).
29. D. Bogert et al., Phys. Rev. **D16**, 2098 (1977).
30. G. A. Alves et al., E769 Collaboration, Phys. Lett. **B559**, 179 (2003); hep-ex/0303027.
31. E. M. Aitala et al., E791 Collaboration, Phys. Lett. **B496**, 9 (2000); hep-ex/0009016.
32. A. E. Brenner et al., Phys. Rev. **D26** (1982) 1497.